Thin Solid Films 517 (2008) 994–999

Contents lists available at ScienceDirect

Thin Solid Films

journal homepage: www.elsevier.com/locate/tsf

Electrical and dielectrical properties of tantalum oxide films grown by Nd:YAG laser assisted oxidation

G. Aygun [a,*], R. Turan [b]

[a] Department of Physics, İzmir Institute of Technology, Gulbahce Campus, TR-35430, Urla-İzmir, Turkey
[b] Department of Physics, Middle East Technical University, TR-06531, Ankara, Turkey

ARTICLE INFO

Article history:
Received 23 March 2007
Received in revised form 23 July 2008
Accepted 30 July 2008
Available online 3 August 2008

Keywords:
Dielectric properties
Electrical properties
Insulators
Metal Oxide Semiconductor structure
Oxidation
Tantalum oxide
Ellipsometry
Fourier Transform Infrared Spectroscopy (FTIR)

ABSTRACT

Tantalum pentoxide (Ta_2O_5) thin films (20 to 44 nm) have been grown by 1064 nm Nd:YAG laser oxidation of Ta deposited films with various thickness on Si. Fourier Transform Infrared (FTIR) spectrum, thickness distribution, dielectric and electrical properties of laser grown oxide layers have been studied. The effect of the sputtered Ta film thickness, laser beam energy density and the substrate temperature on the final Ta_2O_5 film structure has been determined. It is shown that the oxide layers obtained for the laser beam energy density in the range from 3.26 to 3.31 J/cm^2 and the substrate temperature around 350 °C have superior properties. FTIR measurement demonstrates that the Ta_2O_5 layers are obtained with the laser assisted oxidation technique. Metal Oxide Semiconductor capacitors fabricated on the grown oxide layers exhibits typical Capacitance–Voltage, Conductance–Voltage and Current–Voltage characteristics. However, the density of oxide charges is found to be slightly higher than the typical values of thermally grown oxides. The conduction mechanism studied by Current–Voltage measurements of the capacitors indicated that the current flow through the oxide layer is modified Poole–Frenkel type. It is concluded that the Ta_2O_5 films formed by the technique of Nd:YAG laser-enhanced oxidation at relatively low substrate temperatures are potentially useful for device applications and their properties can be further improved by post oxidation annealing processes.

© 2008 Elsevier B.V. All rights reserved.

1. Introduction

To overcome the scaling limit of microelectronic device dimensions, Si-based dielectric materials need to be replaced by advanced high permittivity (high-κ) materials. Therefore, there has been a great demand lately for alternative gate dielectrics [1–3]. Among the high-κ materials like ZrO_2, HfO_2, Ta_2O_5, Y_2O_3, TiO_2 metal oxides, Ta_2O_5 is one of the most promising candidates to replace SiO_2 as a memory dielectric in storage capacitors, since it has excellent step coverage characteristics, high dielectric constant greater than 20 (depending on the conditions during growth), high breakdown field, relatively low leakage currents resulting in a high storage charges and chemically stable structure [2–7].

There are a number of ways to fabricate Ta_2O_5 such as chemical vapor deposition techniques, sputtering, evaporation, sol–gel methods, atomic layer deposition, ion-assisted deposition, laser oxidation of Ta layer [6,7]. Fabrication method strongly affects the structural and electrical properties of grown Ta_2O_5 layers [7]. However, the best production method in terms of storage capacitor applications is not yet clear.

Being a local and low temperature process, laser assisted oxidation is a challenging, but promising approach for the production of future devices and, therefore, it can be used as an alternative technique to produce high-κ oxides [8,9]. The oxide layer fabricated in this way needs to be studied in terms of mainly electrical properties that are essential for Dynamical Random Access Memory applications. In this work, various aspects of Ta_2O_5 films fabricated by Pulsed Laser Oxidation of radio frequency (rf) sputtered Ta layer, i.e. formation of Ta_2O_5 by laser assisted oxidation, thickness profile of the grown films, and their dielectric and electrical properties with the analysis of leakage current mechanisms have been studied.

2. Experimental procedure

Tantalum films with a thickness of 10, 15 and 20 nm were deposited on Si wafers by rf sputtering of tantalum target (99.99% purity) in an Ar atmosphere. The working gas pressure, rf power density and deposition rate were 3 Pa, 2.2 W/cm^2, 9.3 nm/min, respectively. The substrate was not heated intentionally during the tantalum deposition and presumably remained close to room temperature. Subsequently, the samples were laser oxidized in vacuum chamber. During laser oxidation, the substrate temperature was varied between 250 and 400 °C, the laser beam energy density (laser power) was in the range from 3.21 to 3.36 J/cm^2 per pulse, and

* Corresponding author. Tel.: +90 232 750 77 15; fax: +90 232 750 77 07.
E-mail addresses: aygun@photon.iyte.edu.tr, gulnuraygun@iyte.edu.tr (G. Aygun).

0040-6090/$ – see front matter © 2008 Elsevier B.V. All rights reserved.
doi:10.1016/j.tsf.2008.07.039

the oxygen gas pressure was 123 Pa. The laser beam is scanned on the surface of the sample by means of a computer controlled X–Y scanner system which has a 3 cm converging lens with a focal length of approximately 25 cm generated a 1.8 mm diameter of spot size on the substrate. By means of this X–Y scanner system, the laser light shines on a region on the substrate approximately 4×4 mm^2 and this area can be reduced or increased by software. The details of the laser oxidation system and process parameters can be found elsewhere [8,9].

Following the oxidation process of Ta films, the oxide thickness, *d*, and the refractive index, *n*, of the oxide layers were determined by single wavelength ellipsometer working at 632.8 nm (Rudolph Auto EL II). A Fourier Transform Infrared (FTIR) Spectroscopy (Bruker Equinox 55) was used to determine the chemical composition and structure of the films at the substrate temperature of 350 °C and laser power of 3.3 J/cm^2 pulse.

The electrical characterization of the layers was carried out using Metal Oxide Semiconductor (MOS) capacitors with evaporated Al gate electrodes with an area of 1.96×10^{-3} cm^2. The back side of the wafers was hydrofluoric acid cleaned and covered by Al to form ohmic contact. The dielectric and electrical characteristics of the layers were obtained from the Capacitance–Voltage (*C–V*), Conductance–Voltage (*G–V*), and Current–Voltage (*I–V*) measurements. High frequency regime (1 k, 10 k, 100 k, 1 MHz) was used for the *C–V* and *G–V* measurements and series resistance correction was performed for 100 kHz and 1 MHz *C–V* and *G–V* data. Effective dielectric constant (ε_{eff}), flatband voltage (V_{FB}), different types of oxide charges/charge densities, i.e. Q_f (fixed oxide charges), Q_{sl} (slow states), D_{it} (fast states) and hysteresis effect were extracted from the *C–V* and *G–V* data. Using the *I–V* measurements of the oxide layers, the conduction mechanisms in Ta_2O_5 oxide layer were determined.

3. Results and discussions

3.1. Formation of Ta_2O_5 film

Fig. 1 shows the FTIR spectra of laser oxidized layer produced from initial 10 nm thick Ta film on Si. The spectra correspond to the film obtained at laser beam energy density of 3.3 J/cm^2, the substrate temperature of 350 °C, and the oxide layer thickness of 20 nm. Although the spectra were taken between 400 and 4000 cm^{-1}, the region of 400–1200 cm^{-1} is displayed in the figures only because of the importance of the low wavenumber region (<1100 cm^{-1}) in the detection of the tantalum oxide-related bonds. As evidenced by the weakness of the OH signal around 3300–3400 cm^{-1} of the FTIR spectra, the films are almost moisture-free.

A dominant absorption feature around 650 cm^{-1} and a wide shoulder like absorption band with a small intensity between 450 and 550 cm^{-1} indicate the presence of tantalum oxide(s) in the layers [10,11]. A wide shoulder like absorption peak with a small intensity dip

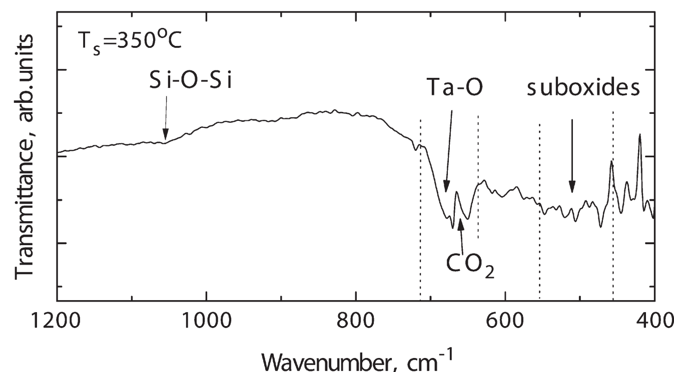

Fig. 1. FTIR spectra of the 20 nm thick oxide grown at the substrate temperature of 350 °C and the laser beam energy density of 3.3 J/cm^2.

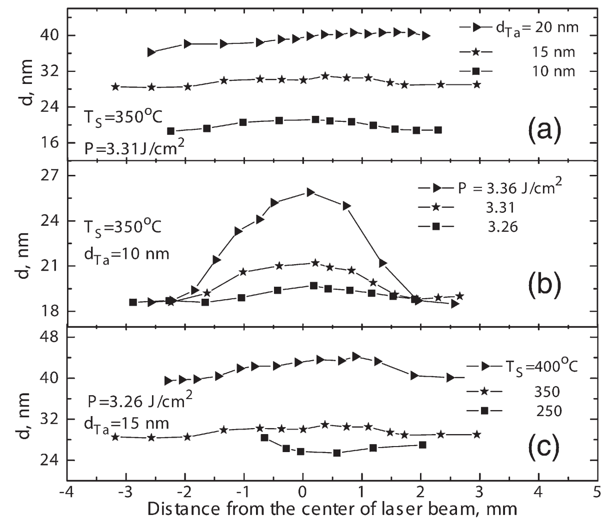

Fig. 2. Oxide thickness distribution profile with respect to the center of the laser beam for the conditions of (a) thickness of rf-sputtered Ta film (b) laser beam energy density (c) substrate temperature.

between 850 and 1000 cm^{-1} is attributed to the presence of very tiny amount of suboxides in the oxidized layer [11]. The feature superimposed on the main broad signal at 670 cm^{-1} is associated with vibration modes of CO_2 resulting probably from the air ambient during the measurements. Since this peak is not related to the oxidation process, we will not discuss it further.

One of the typical features of the high-κ dielectrics grown on Si substrate is that an ultra thin SiO_2 formed at the interface [2,4,5,7]. Although Ta_2O_5 is not an exception, measured spectra did not reveal a strong indication for the presence of Si–O stretching band which is typically around 1070–1100 cm^{-1}. The film has very small bands in this region which can be attributed to the presence of Si–O–Si stretching vibration mode [12]. Based on this observation, one can conclude that interfacial layer containing SiO_2 and/or intermediate oxidation states of Si, is extremely thin if present for this specific film.

3.2. Thickness distribution

This section presents the discussions on the variation of the Ta_2O_5 film thickness with respect to the distance from the center of the laser beam as a function of process parameters like thickness of the sputtered Ta film, laser beam energy density and substrate temperature. Fig. 2(a) represents the effect of Ta film thickness for 10, 15 and 20 nm initial thick rf-sputtered Ta films. The laser beam energy density and the substrate temperature are 3.31 J/cm^2 and 350 °C. The refractive index values of oxides are 1.9, 2.1 and 2.1 for 10, 15 and 20 nm initial thick Ta films respectively and their values are very close to those of bulk Ta_2O_5 (2.1) [3]. The oxide thicknesses being ~22.5 nm, ~32.5 nm and 41.5 nm for initial 10, 15 and 20 nm thick Ta films are in agreement with the expectation of approximately twice that of initial Ta film thickness. It is also seen that the highest value of the oxide thickness, *d*, is measured at the center of the laser beam (denoted by "0" in Fig. 2) and the thickness distribution is approximately uniform across the laser irradiated region. The thickness variation across the oxidized region is more homogenous for initially thicker Ta films and a relatively flat region can be found over the distance of 2 mm at the center of the laser beam, across which the thickness variation is within ~8% for initially 10 nm thick Ta films and 2.2 nm flat region is obtained for the oxides of higher initial thick Ta films.

The impact of laser beam energy density on oxide thickness, *d*, is shown in Fig. 2(b). The substrate temperature and the initial Ta film thickness were 350 °C and 10 nm during the oxidation, respectively. The refractive index values are 1.9, 1.9 and 2.2 corresponding to laser

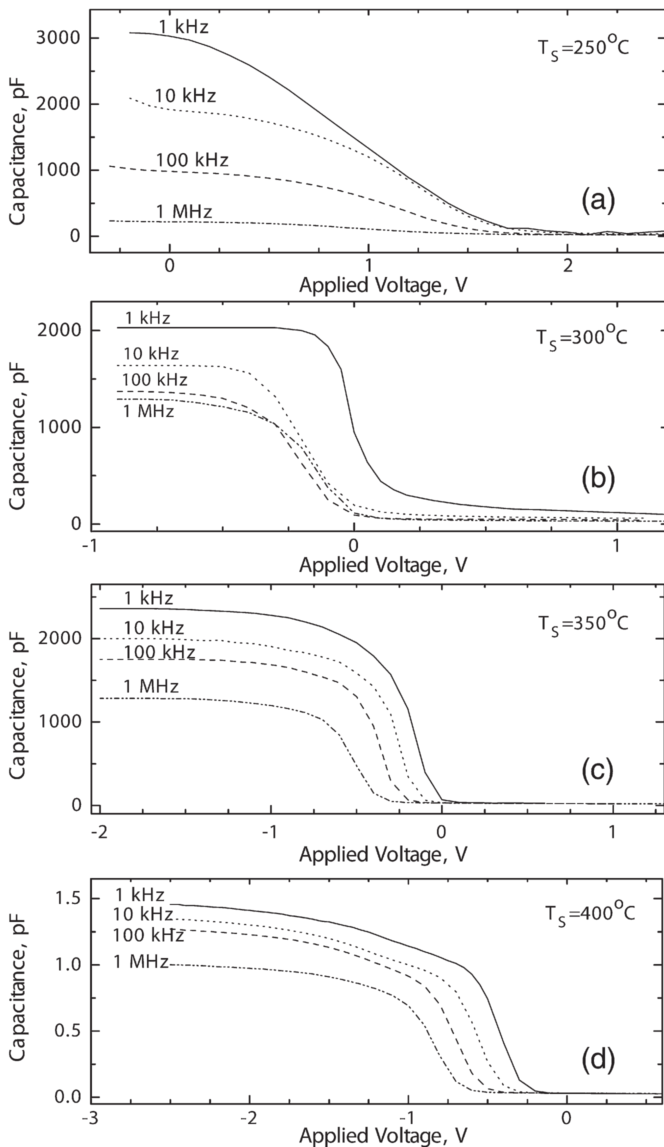

Fig. 3. *C–V* curves measured at different frequencies (1, 10, 100, 1000 kHz) for 21 nm thick film produced at (a) 250 °C (b) 300 °C (c) 350 °C (d) 400 °C.

power of 3.26, 3.31 and 3.36 J/cm^2. The refractive index being 2.2 for 3.36 J/cm^2 is close to that of bulk Ta_2O_5. The lateral variations of oxide thicknesses are all Gaussian-like and their values at the center are close to each other for the lower two laser powers, namely ~19.5 nm for 3.26 J/cm^2 and 21 nm for 3.31 J/cm^2, but it increases up to 26 nm for the laser power of 3.36 J/cm^2 having a relatively narrow Gaussian thickness profile. The thickness variation is obtained around 1.4% for P=3.26 and 3.31 J/cm^2 while it increases little bit more to ~1.7% for P=3.36 J/cm^2 over the distance of 1 mm from the laser beam center. These results show that the expected oxide thickness, approximately twice that of initial Ta film, is obtained at relatively lower laser powers, i.e. 3.26–3.31 J/cm^2, while it increases up to ~2.5 times that of initial thick Ta film for the laser power of 3.36 J/cm^2. This could be due to the fact that a SiO_2 layer is formed at the interface between Ta_2O_5 and Si substrate as a result of higher laser power. Presence of SiO_2 layer at the interface is undesirable because of its effect on the effective dielectric constant of the oxide layer. On the other hand, Ta may not be totally oxidized for lower laser energy fluences [9]. An optimum interval for the laser power should exist for uniform oxidation. In the present case, most uniform oxide layers were obtained at the laser power ranging from 3.26 to 3.31 J/cm^2 per pulse.

The effect of the substrate temperature on the thickness distribution of the Ta_2O_5 layers is given in Fig. 2(c). The thickness of the initial Ta film and the laser power were 15 nm and 3.26 J/cm^2, respectively. It is obvious that all curves have a Gaussian shape and the thickness variation over 1 mm at the center of the oxidized region changes between 0.5% and 0.7% which is very low. The maximum oxide thickness measured at the center of the laser oxidized region is around 25.5 nm for 250 °C, 31 nm for 350 °C and 44 nm for 400 °C. The ideal thick oxide for 15 nm thick Ta film is obtained around 350 °C. However, for T_s=250 °C, the oxide thickness (lower than expected value) has an opposite shape of Gaussian thickness distribution, namely the lowest thickness at the center and then sudden increase at the periphery, which indicates that the layer is mostly metallic in the periphery while a slightly oxidized region is at the center. The refractive index values were measured to be 2.1 and 2.0 respectively for 350 °C and 400 °C. Since the oxide layer thickness for 400 °C increases suddenly to about 44 nm while the expected value is 30 nm, and the refractive index value is lower than that of 350 °C, it can be concluded that the Si substrate at the interface is also oxidized containing the suboxide forms of Si, Ta and O in addition to the oxidation of the Ta film.

Oxide growth conditions affect the crystallinity of the grown films. This situation was examined for various growth conditions of Nd:YAG laser oxidized tantalum films in our earlier publication. X-ray diffraction data showed that the films grown at or below 350 °C are amorphous while the films grown at higher temperature are polycrystalline with orthorhombic structure [9].

3.3. Dielectric and electrical parameters

In this section, the electrical properties, i.e. *C–V*, *G–V* and *I–V* of 4 samples produced at T_s=250, 300, 350, 400 °C are presented. *C–V* curves were taken at high frequencies namely 1 kHz, 10 kHz, 100 kHz, 1 MHz for MOS capacitors with 1.96×10^{-3} cm^2 Al gate area. Series resistance corrections were applied to 100 kHz and 1 MHz *C–V* and *G–V* data. High frequency *C–V* and *G–V* data have been analyzed to obtain ε_{eff}, V_{FB}, Q_f, Q_{sl}, and D_{it}. Fig. 3(a–d) shows *C–V* curves with accumulation, depletion and inversion regions after the series resistance correction has been applied. However, the frequency dispersion seen in the accumulation part of the *C–V* curves indicates that the series resistance effect cannot be eliminated totally. This effect is more visible in the high frequency regimes as expected [13].

The ε_{eff} of the oxide layers (21 nm thick) was determined from the capacitance value at accumulation mode of 1 MHz, 100 kHz, 10 kHz and 1 kHz *C–V* curves of the MOS structure. The ε_{eff} values corresponding to each high frequency *C–V* curve are given in Table 1 for all samples at the given substrate temperatures, and seen that almost

Table 1
Dielectric and electrical properties obtained from capacitance and conductance with respect to voltage graphs

	f, kHz	T_s, °C			
		250	300	350	400
ε_{eff}	1	37.13	23.22	28.50	17.64
	10	22.61	19.78	23.90	15.99
	100	11.77	14.42	17.00	15.42
	1000	2.81	15.33	15.10	12.16
V_{FB}, V	1	1.34	0.056	−0.014	−0.32
	10	1.36	−0.040	−0.084	−0.46
	100	1.28	−0.172	−0.203	−0.59
	1000	1.08	−0.017	−0.371	−0.71
Q_f 10^{12} cm^{-2}	1	−19.96	−4.625	−5.171	−1.767
	10	−12.31	−3.442	−3.947	−1.059
	100	−6.15	−2.007	−2.789	−0.444
	1000	−0.79	−2.763	−1.345	0.037
D_{it} 10^{12} cm^{-2} eV^{-1}	1000	1.6	1.5	2.1	2.4
Q_{sl} 10^{11} cm^{-2}	1000	−1.48	2.07	4.18	3.846

all ε_{eff} values are higher than that of ideal SiO_2 (ε_{SiO_2}=3.9). Since accumulation capacitance (C_{acc}) values depend on the frequency (Fig. 3a–d), so do ε_{eff} values. The ε_{eff} values of grown oxide films change between 12 and 15 at 1 MHz frequency limit except that for T_s=250 °C oxide. The ε_{eff} values determined from these measurements are comparable to the values of oxides grown by other techniques [4,7]. For lower frequencies, the corresponding ε_{eff} values increase as a result of the increment in the accumulation capacitance values as frequency decreases.

Our recent results [9] support that the effective oxidation temperature for Ta films starts somewhere in between 300 °C and 350 °C. For the lowest T_s, 250 °C, the ε_{eff} is too much variable with respect to frequency showing that the grown layer is not uniform. The calculated ε_{eff} data for 300 °C and 350 °C are reliable, and ε_{eff} values are comparable to the results of other groups using different growth techniques [4,7]. However, the decrease in ε_{eff} values when T_s increases to 400 °C is an evidence that a SiO_2 layer is formed at the interface [9] resulting in a smaller ε_{eff} value when the substrate temperature exceeds a certain value.

The Q_f values are calculated from the shift in V_{FB} which is obtained from the position at the conduction peak together with work function difference between Al gate and Si (−0.7 eV) (Table 1). The Q_f at 1 MHz frequency is found to be ~0.4×10^{11} cm^{-2} for T_s=400 °C, whereas it changes from ~(-7.9×10^{11} cm^{-2}) to ~(-27.6×10^{11} cm^{-2}) for T_s=250–350 °C oxides. The Q_f values calculated for laser grown oxides are approximately one order higher than those of common production methods of Ta_2O_5 films [4] and this behavior of Q_f is generally associated with structural imperfections, bond defects and poor oxidation process. In addition, the fixed oxide charges often originate from the incomplete chemical bonding of the atoms near the dielectric/semiconductor interface [6]. One particular example for these electrically active defects in Ta_2O_5 is the oxygen vacancies [4].

Laser grown oxides exhibit hysteresis at 1 MHz *C–V* curves when the gate voltage is swept from accumulation to inversion and then from inversion to accumulation. This indicates the presence of slow states, Q_{sl}, which are located very close to the Si/oxide interface (Table 1). The shift in the *C–V* curves at the flat band voltage value, ΔV_{hyst}, at 1 MHz *C–V* curve changes between −51 mV and −120 mV giving rise to $2.1–4.2\times10^{11}$ cm^{-2} slow states for the substrate temperatures, T_s=300–400 °C. For the lowest substrate temperature, i.e. T_s=250 °C, Q_{sl} is obtained as -1.5×10^{11} cm^{-2} (ΔV_{FB}^{hyst}=0.200*V*). These values are comparable to those obtained by other groups [4].

The D_{it} values were calculated using Terman method [13,14]. At high frequencies ($\omega\tau\gg1$), interface traps cannot follow the ac voltage swing, which yields the high frequency curve, free of capacitance due to interface traps. As a result, *C–V* curve at high frequencies has a stretch out with respect to low frequency regime due to interface trap charges. Terman method uses the distortion of high frequency *C–V* curves caused by the existence of interface charges to calculate D_{it} value using;

$$D_{it}(\Psi_S)=\frac{C_{it}(\Psi_S)}{q}=\frac{1}{q}\left[C_{ox}\left(\left(\frac{d\Psi_S}{dV_G}\right)^{-1}-1\right)-C_S\right] \quad (1)$$

where C_S is the surface capacitance of silicon, ψ_S is the surface band bending of silicon, and q is the elementary charge. By comparing the experimental and theoretical ($d\psi_S/dV_G$), one can obtain the D_{it} of the *C–V* curves [13].

The values of D_{it} as found from 1 MHz *C–V* curves are obtained in the range between 1.5×10^{12} and 2.4×10^{12} cm^{-2} eV^{-1} (Table 1). These values are comparable to the values obtained from the other oxide growth methods [4,14].

3.4. I–V characteristics of the capacitors

Fig. 4 shows the leakage current density, *J*, measured through the Al–Ta_2O_5–Si capacitors as a function of applied voltage for substrate temperatures, T_s, of 300, 350, 400 °C. The effective oxide thickness values measured by the ellipsometry are given as (a) 21 nm and (b) 39 nm. Since the oxide quality for the substrate temperature of 250 °C and lower T_s levels is not enough, *I–V* characteristics were not examined for this sample. It is apparent from the comparison of Fig. 4 (a) and (b) that the leakage current density decreases by two orders of magnitude with increasing oxide thickness indicating that electrically and stoichiometrically better oxide layers are obtained for the thicker films formed at higher substrate temperatures. The leakage current density for 39 nm oxide is very low being in the range of 10^{-9} A/cm^2, however, it is around 10^{-7} A/cm^2 for 21 nm thick oxide.

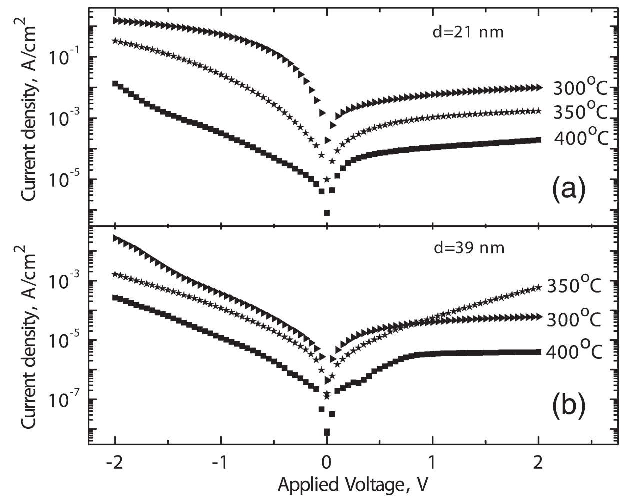

Fig. 4. The leakage current density versus applied voltage for T_s=300 °C, 350 °C, 400 °C (a) d_{oxide}=21 nm (b) d_{oxide}=39 nm.

The variations of the current density in the forward bias conditions (negative applied voltage values for which electrons are injected from the Al gate for p-type Si) is small for 300 °C to 350 °C while there is a sharp decrease from 350 °C to 400 °C, indicating formation of a better insulation in the samples oxidized at higher temperatures. Although the leakage current density decreases with increasing T_s in most cases, it shows an abnormal increase in the reverse bias part of the *I–V* curve of the sample formed at 350 °C (Fig. 4(b)). This could result either from the pin-holes present in the grown oxide or from the undesired contact of the MOS electrode to the regions where the grown oxide has poor quality.

Lower ε_{eff} value for the films grown at higher temperatures (400 °C) indicates the presence of a SiO_2 interfacial layer between Si substrate and Ta_2O_5. This layer might play an important role in the variation of the current density. When a sufficiently thick interfacial SiO_2 is formed, it may dominate the current flow through the oxide [7]. The decrease in *J* with increasing T_s can then be explained with the less amounts of defects (such as dangling bonds or lack of oxygen) in the oxide structure of the films and formation of SiO_2 interfacial layer which provides better barrier for electrical conduction.

3.5. Conduction mechanisms

The current flow through the Ta_2O_5 films can be described by using various conduction mechanisms whose importance vary with the electric field. These are (i) electronic hoping conduction, (ii) field assisted emission, (iii) Poole–Frenkel (PF) effect, (iv) double barrier tunneling, (v) direct tunneling, (vi) Fowler–Nordheim tunneling (vii) Schottky emission (SE) [15]. One or more of these mechanisms can be applied depending on various device and measurement parameters [2,15,16]. The conduction in thin Ta_2O_5 films has been generally interpreted by two d.c. conduction mechanisms, i.e. SE which is electrode limited or PF which is bulk limited mechanisms

[17]. It was reported that the conduction mechanism is strictly bulk limited for thermally oxidized Ta_2O_5 films, while it is, electrode limited especially at low voltages for highly imperfect films having large numbers of oxygen deficiencies [18,19].

Because of the non-uniformity in the oxides grown by laser oxidation, the major dominating current type is hard to determine. However, the analysis have strongly indicated that the conduction mechanism through the laser grown Ta_2O_5 films in the applied voltage ranges is governed by the PF in the samples having a barrier height separating the traps from the conduction band. PF is based on the emission of trapped electrons toward the conduction band of the insulator [20,21]. Current density governed by the PF mechanism through the dielectric is given as [22];

$$J_{\mathrm{PF}} = \mathrm{CE}\exp\left[\frac{q}{k_{\mathrm{B}}T}\left(-\Phi_0 + \frac{1}{r}\left(\frac{qE}{\pi\varepsilon_0 K_{\mathrm{r}}}\right)^{1/2}\right)\right] \quad (2)$$

where J_{PF} is the current density, C is the temperature dependent constant related to the density of trapping centers, E is the electric field in Ta_2O_5, q is the electronic charge, Φ_0 is the barrier height separating the traps from the conduction band, k_{B} is the Boltzmann constant, T is the absolute temperature, ε_0 is the permittivity of free space, and K_r is the high frequency dynamic dielectric constant, that is equal to the square of the refractive index. r is a degree of compensation whose value changes between 1 and 2 ($1 \le r \le 2$) [20,21], and it defines the effect of trapping or acceptor sensors. When r is equal to 1, then it is named as normal PF, while it corresponds to modified Poole–Frenkel effect or Poole–Frenkel with compensation when r=2. If the plot of $\ln(J/E)$ versus $E^{1/2}$ results in a straight line, it suggests that the conduction is dominated by PF mechanism and $r\sqrt{K_r}$ value can be extracted from the measured curve. Since r changes between 1 and 2, and K_r is the square of refractive index value, then the range for $r\sqrt{K_r}$ can be counted as normal when its value is between 1.9 and 4.5.

Fig. 5 shows $\ln(J/E)$ versus $E^{1/2}$ plot with fitting lines Eq. (2) of laser oxidized Ta_2O_5 layers for 300, 350 and 400 °C for (a) 21 nm, and (b) 39 nm oxide. The calculated $r\sqrt{K_r}$ values at the given substrate temperatures from the fitted lines is shown in Table 2. It is known that formation of a very thin layer of suboxides containing Si, Ta and O is inevitable in most cases [4,7]. Based on the spectroscopic reflectance measurements [23] and XPS (X-ray Photoelectron Spectroscopy) depth profiling results of laser oxidized SiO_2 layers [24], it is again expected that the laser oxidized Ta_2O_5 layers could have suboxide layer at the interface. Since the refractive index and thickness measured by single wavelength ellipsometer (632.8 nm) are not reliable without other independent measurements, extraction of r from K_r is not possible and therefore $r\sqrt{K_r}$ values are listed in Table 2. However, monotonic increase in the $r\sqrt{K_r}$ values can be attributed to the densification in the film structure. The refractive index is expected to increase as a result of reducing the amount of suboxides with increasing substrate temperature T_s [23]. The increase with respect to T_s increment in the measured $r\sqrt{K_r}$ values can be extracted from Fig. 5 for both oxide thicknesses. The dependence of n on T_s at 633 nm wavelength for a constant laser power was presented in our earlier work [9], where it was confirmed that n increases with respect to T_s increment and reaches similar values reported for as-fabricated Ta_2O_5 films obtained by other methods [4,7]. One can conclude that increasing substrate temperature, T_s, results in formation of denser Ta_2O_5 oxide layers with higher refractive index $(n = \sqrt{K_r})$ [9], with less number of defects in or at the interface of the grown films.

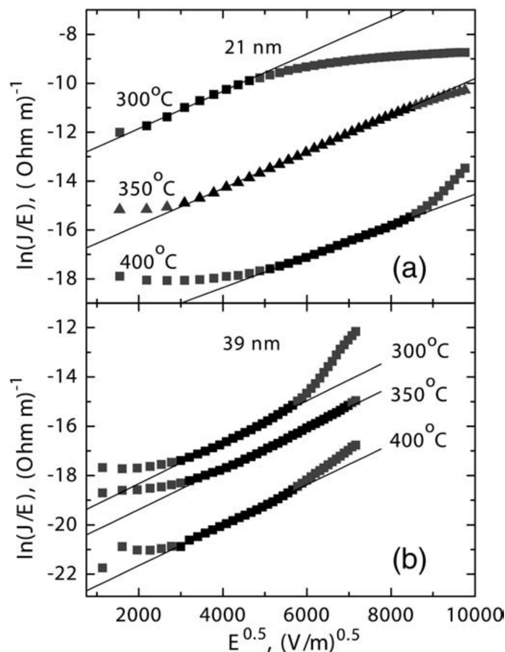

Fig. 5. ln (J/E) versus $\sqrt{E}$ for laser oxidized Ta_2O_5 layers grown at T_s=300 °C, 350 °C, 400 °C for the oxide thicknesses of; (a) d_{oxide}=21 nm (b) d_{oxide}=39 nm.

Table 2
Poole–Frenkel conduction mechanism constants, $r\sqrt{K_r}$, for 21 and 39 nm oxides with respect to substrate temperature

	$r\sqrt{K_r}$		
	300 °C	350 °C	400 °C
21 nm oxide	3.83	3.91	4.60
39 nm oxide	3.48	3.53	3.57

When I–V curves are analyzed by applying PF formalism, we observe a general agreement in some part of the curves as seen in Fig. 5. It is clear from the experimental curves that more than one conduction mechanisms might be important for the current flow through these samples.

The presence of interfacial SiO_2 layer affects the characteristics of the MOS devices. First of all, the overall effective dielectric constant of the insulating system is reduced. Second effect of the SiO_2 layer would be an increase in the overall resistance of the grown layer. For a complete analysis, the interfacial SiO_2 should be taken into account. Assuming that the accumulated charge at the Ta_2O_5/SiO_2 interface is zero, the electric field distribution within the oxide layer (Ta_2O_5/SiO_2) is determined by

$$\varepsilon_{\mathrm{T}} E_{\mathrm{T}} = \varepsilon_{\mathrm{S}} E_{\mathrm{S}} \quad (3)$$

where ε_{T}, ε_{S} are the permittivity of Ta_2O_5 and SiO_2, and E_{T} and E_{S} are electric field across the Ta_2O_5 and SiO_2 layers respectively. Then, applied voltage across the oxide layer (Ta_2O_5/SiO_2) can be given by the following expression:

$$V = E_{\mathrm{T}} d_{\mathrm{T}} + E_{\mathrm{S}} d_{\mathrm{S}} \quad (4)$$

where d_{S} and d_{T} are the oxide thicknesses of SiO_2 and Ta_2O_5 layers. From the given equations, the electric field across the SiO_2 and Ta_2O_5 can be obtained as;

$$E_{\mathrm{S}} = \frac{V}{\frac{\varepsilon_{\mathrm{S}}}{\varepsilon_{\mathrm{T}}} d_{\mathrm{T}} + d_{\mathrm{S}}} \quad (5)$$

$$E_{\mathrm{T}} = \frac{V}{\frac{\varepsilon_{\mathrm{T}}}{\varepsilon_{\mathrm{S}}} d_{\mathrm{S}} + d_{\mathrm{T}}}. \quad (6)$$

Since the thickness of SiO_2 is in the range of 2 nm and that of Ta_2O_5 is around 20 nm, it is found that the E field on SiO_2 is much higher than on Ta_2O_5 Eqs. (5) and (6). On the other side, because of the difference in the bandgap of Ta_2O_5 (~5 eV) and SiO_2 (~9 eV), charge

carriers are accumulated at the Ta_2O_5/SiO_2 interface and therefore the breakdown probability of SiO_2 is high. When the top electrode is positively biased for a system of metal/Ta_2O_5/SiO_2/p-Si, electrons are injected from the substrate into the SiO_2 layer and tunnel through the impurity levels in the Ta_2O_5 or trapped at the SiO_2/Ta_2O_5 interface. In the reverse bias situation, i.e. when the gate is negatively biased, electrons are injected from the metal gate. If the formation of SiO_2 layer could be avoided, we might expect lower electric field across the insulator resulting in a reduced leakage current.

4. Conclusions

It has shown that Ta_2O_5 films with good quality can be grown by Nd:YAG laser oxidation (λ = 1064 nm) at low temperatures. Best process conditions in terms of laser power and substrate temperatures were determined. The FTIR analyses and refractive index values (~1.9–2.2) show that laser grown layers have good qualities being close to those of bulk Ta_2O_5. The oxide charges for the best oxides were found to be in the same range as those obtained by other technologies. The leakage current density, *J*, through the oxide decreased with the increment in the oxide thickness and the substrate temperature. The conduction mechanism is governed by the modified Poole–Frenkel mechanism in a wide region of the *I*–*V* curve.

Even though promising results were obtained from Nd:YAG laser oxidation of Ta films on Si, the electrical properties and uniformity of the films can further be improved by optimizing the process conditions and post oxidation processes. The best conditions for Nd:YAG laser oxidation of Ta films are 300 and 350 °C for T_s, and 3.3 J/cm^2pulse for laser beam energy density. In order to decrease the porosity, so do increase the refractive index of the films, post annealing procedure in vacuum can be applied to obtain denser layers.

Current mechanisms need to be studied in details with low temperature measurements and activation analysis as a forthcoming duty. Future work will focus on the given issues as well as more detailed structural analysis and interfacial properties of the grown film with respect to XPS depth profile analysis and additionally Transverse Electron Microscope cross sectional pictures.

Acknowledgements

This work has been supported by TUBITAK (Scientific and Technical Council of Turkey) under project number TBAG/U68. The authors would like to thank Prof. D. Sc. Elena Atanassova from Institute of Solid State Physics of Bulgarian Academy of Sciences for her excellent and valuable comments.

References

[1] S. Sayan, E. Garfunkel, S. Suzer, Appl. Phys. Lett. 80 (2002) 2135.
[2] Intern. Techn. Roadmap for Semiconduct. (ITRS) 2004 edition, http://public.itrs.net, last accessed date April 2008.
[3] L. Manchanda, M.D. Morris, M.L. Green, R.W. van Dover, F. Klemens, T.W. Sorsch, P.J. Silverman, G. Wilk, B. Busch, S. Aravamudhan, Microelectron. Eng. 59 (2001) 351.
[4] E. Atanassova, Microelectron. Reliab. 39 (1999) 1185.
[5] A.I. Kingon, J.P. Maria, S.K. Streiffer, Nature 406 (2000) 1032.
[6] G.D. Wilk, R.M. Wallace, J.M. Anthony, J. Appl. Phys. 89 (2001) 5243.
[7] C. Chaneliere, J.L. Autran, R.A.B. Devine, B. Balland, Mater. Sci. Eng. R22 (1998) 269.
[8] G. Aygun, E. Atanassova, A. Alacakir, L. Ozyuzer, R. Turan, J. Phys. D: Appl. Phys. 37 (2004) 1569.
[9] E. Atanassova, G. Aygun, R. Turan, Tz. Babeva, J. Vac. Sci. Technol. A 24 (2006) 206.
[10] I.W. Boyd, J.Y. Zhang, Microelectron. Reliab. 40 (2000) 649.
[11] J.J. Yu, J.Y. Zhang, I.W. Boyd, Appl. Surf. Sci. 186 (2002) 57.
[12] J.Y. Zhang, Q. Fang, I.W. Boyd, Appl. Surf. Sci. 138–139 (1999) 320.
[13] E.H. Nicollian, J.R. Brews, MOS (Metal Oxide Semiconductor) Physics and Technology, John Wiley and Sons, New-York NY, 1982.
[14] H.P. Lin, J.G. Hwu, IEEE Trans. Electron Dev. 54 (2007) 3064.
[15] C. Chaneliere, J.L. Autran, R.A.B. Devine, J. Appl. Phys. 86 (1999) 480.
[16] P.M. Campbell, E.S. Snow, Mater. Sci. Eng. B 51 (1998) 173.
[17] S. Ezhilvalavan, T.Y. Tseng, J. Mater. Sci.: Mater. Electron. 10 (1999) 9.
[18] P.L. Young, J. Appl. Phys. 47 (1976) 235.
[19] P.L. Young, J. Appl. Phys. 47 (1976) 242.
[20] John G. Simmons, Phys. Rev. 155 (1967) 657.
[21] J.R. Yeargan, H.L. Taylor, J. Appl. Phys. 39 (1968) 5600.
[22] C. Chaneliere, S. Four, J.L. Autran, R.A.B. Devine, Microelectron. Reliab. 39 (1999) 261.
[23] G. Aygun, E. Atanassova, R. Turan, Tz. Babeva, Mater. Chem. Phys. 89 (2005) 316.
[24] G. Aygun, E. Atanassova, K. Kostov, R. Turan, J. Non-Cryst. Solids 352 (2006) 3134.